

# A Novel Positioning-Communication Integrated Signal in Wireless Communication Systems

Lu Yin<sup>ID</sup>, *Member, IEEE*, Jiameng Cao, Kaiqin Lin, Zhongliang Deng, and Qiang Ni<sup>ID</sup>, *Senior Member, IEEE*

**Abstract**—We propose a novel positioning-communication integrated signal, which superposes the configurable positioning signal on the communication one to achieve a sub-meter range measurement accuracy. Different from other positioning schemes, there are multi positioning signals on different sub-carriers for different positioning users. The powers and bandwidths of these positioning signals are controllable, which reduces the near-far effect, and improves the range measurement accuracy. Other major contributions are: we analyze the interference of the positioning signal to the communication one; we give the lower-bound and measurement accuracy of the range estimation in both flat and fading channels, and derive their simple expressions. The results show the interaction between the communication and positioning signals is limited, and it is feasible to use the proposed signal for high accuracy positioning.

**Index Terms**—Positioning-communication integrated signal, MS-NOMA, interference, positioning.

## I. INTRODUCTION

NOWADAYS, the ubiquitous positioning has been paid much attention. The satellite positioning systems can not be used indoors as their signals are easily blocked by buildings [1]. Wi-Fi, Bluetooth or Wireless Sensor Networks (WSN) based positioning have a well coverage indoors only with dense placements of the nodes. And it is costly for collecting and maintaining the fingerprint database [2]. Wireless communication network has a well coverage both indoors and outdoors. Meanwhile, it is cost-effective to be used for positioning purpose as it is ready-made for communication purpose.

Specific Positioning Reference Signal (PRS) is designed in 4G network. However, the positioning accuracy of PRS is only tens of meters as the discontinuous signal is hardly tracked which leads a low range measurement accuracy [3]. Moreover, there are severe near-far effects between the positioning signals from different BSs which makes the signals from far BSs more difficult to be received [4]. Consequently,

poor geometric distribution of BSs is achieved which further worsen the positioning accuracy.

Different from all other existing works, we aim to develop a new signal to overcome the aforementioned drawbacks which makes the communication network have the ability of high accuracy positioning. The new signal must satisfy the following requirements:

- 1) The powers of the positioning signal to different users should be controllable to receive more signals and reduce the near-far effect, i.e., different users should obtain different signal strengths or gains from one BS.
- 2) The positioning signal should be continuous, i.e., the receiver can track the signal for better measurement accuracy.
- 3) The interferences between the positioning and communication signals must be weak enough. In fact, notice that the PRS occupies some sub-carriers of 4G signal, we consider PRS is also an interference to the 4G communication signal as it results in a resource reduction for communication.

The main contributions of this letter are:

- 1) We propose a novel positioning-communication integrated signal, called Multi-Scale Non-Orthogonal Multiple Access (MS-NOMA), which integrates positioning and communication signals together without much interference. Contrary to the PRS in 4G, MS-NOMA does not occupy the communication sub-carriers/resources. The positioning signals are superposed upon the communication signals. To avoid interferences, the positioning signals are weak enough and pseudorandom codes are employed to obtain the spreading gains. So that the Successive Interference Cancellation (SIC) in normal NOMA demodulation is unnecessary [5].

- 2) Interferences between the positioning and communication signals are analyzed. Bit Error Rate (BER) for communication and the range measurement accuracy for positioning in both flat and fading channels are derived, respectively. According to these, the feasibility of the MS-NOMA are studied.

## II. THE PROPOSED MULTI-SCALE NON-ORTHOGONAL MULTIPLE ACCESS

Consider a traditional NOMA signal, such as  $y = \sqrt{2P_1}x_1 + \sqrt{2P_2}x_2$  for two-users, where  $x_i$  and  $P_i$  ( $i = 1, 2$ ) are the signal and power of User $i$ , respectively. We usually have  $P_1 \gg P_2$ , so  $x_2$  is seen as a noise to  $x_1$  which can be detected directly. Then, SIC is usually employed to detect  $x_2$  by subtracting  $x_1$ .

The proposed MS-NOMA architecture consists of two kinds of signals: communication and positioning signals as shown in Figure 1. Different from NOMA, both of the communication and positioning signals are Orthogonal Frequency Division Multiple Access (OFDMA) system for different users. And

Manuscript received March 21, 2019; revised May 11, 2019; accepted May 14, 2019. Date of publication May 21, 2019; date of current version October 11, 2019. This work was supported in part by the National Natural Science Foundation of China under Grant 61801041, in part by the Key Research and Development Program of China under Grant 2016YFB0502001, and in part by the Royal Society Project under Grant IEC170324. The associate editor coordinating the review of this paper and approving it for publication was B. Makki. (*Corresponding author: Lu Yin.*)

L. Yin, J. Cao, K. Lin, and Z. Deng are with the School of Electronic Engineering, Beijing University of Posts and Telecommunications, Beijing 100876, China (e-mail: inlu\_mail@bupt.edu.cn; caojiameng@bupt.edu.cn; linkaiqin@bupt.edu.cn; dengzhl@bupt.edu.cn).

Q. Ni is with the InfoLab21, School of Computing and Communications, Lancaster University, Lancaster LA1 4WA, U.K. (e-mail: q.ni@lancaster.ac.uk).

Digital Object Identifier 10.1109/LWC.2019.2917670

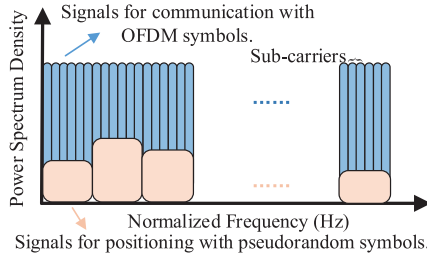


Fig. 1. The proposed MS-NOMA architecture.

the pseudorandom codes are modulated over the positioning sub-carriers for spreading gains and range measuring. Note C-User and P-User as the communication and positioning users, respectively. Let us define  $B$  as the total bandwidth.  $\Delta f_c$  and  $\Delta f_p$ , which are designed as  $\Delta f_p = G\Delta f_c$ ,  $G \in \mathbb{N}_+$ , are the carrier spacing of the communication and positioning signals, respectively. We assume both C-User and P-User occupy an own separate sub-carrier so that there are maximum  $N = B/\Delta f_c - 1$  and  $M = B/\Delta f_p - 1$  users for communication and positioning purpose, respectively.

Different from traditional positioning scheme, there are multi positioning signals broadcast from one BS for different P-Users. Then, specific power control strategy can be used for different P-Users with different channel states which will satisfy the first requirement in Section I. On the other hand, MS-NOMA superposes the spreading sequences in time domain to ensure range measuring which satisfies the second requirement in Section I.

Notice that the positioning signals located on different sub-carriers are orthogonal, so there is no interference between P-Users. However, like the normal NOMA signals, there are interferences between the communication and positioning signals analyzed as follows.

### III. INTERFERENCE ANALYSIS

#### A. Interference of the Positioning Signal to Communication One

The superposed positioning signal can be seen as a noise that interferes the detection of communication signal. Without any loss of generality, we assume the powers for all C-Users are identical. We use BER to evaluate the interference under the assumption that each spreading sequence for different P-Users is independent [6], [7]:

$$BER(n) = K \operatorname{erfc} \left( \frac{\lambda P_c T_c}{I(n) + 2N_0} \right) \quad (1)$$

where  $n$  represents the index of C-User.  $K$  and  $\lambda$  are determined by the modulation and coding schemes.  $P_c$  is the power of the communication signal.  $T_c$  is the period of the communication symbol.  $N_0$  is the environment noise's single-sided Power Spectral Density (PSD).  $I(n) = \sum_{m=1}^M \bar{P}_{p,m}(n)$  represents the interference of the positioning signal to the  $n^{\text{th}}$  C-User. Where  $m$  represents the index of P-User, and  $\bar{P}_{p,m}(n)$  is the power of the  $m^{\text{th}}$  P-User over the  $n^{\text{th}}$  C-User which satisfies:

$$\bar{P}_{p,m}(n) = P_{p,m} G_{p,m}(n\Delta f_c) = P_{p,m} T_p \operatorname{sinc}^2 \left( m - \frac{n}{G} \right) \quad (2)$$

where  $P_p$  is the power of the positioning signal.  $T_p$  is the period of the positioning symbol.  $G_{p,m}(f) = T_p \operatorname{sinc}^2[(f - m\Delta f_p)T_p]$  is the normalized PSD of the  $m^{\text{th}}$  positioning signal.

In the multi-path scenario, the powers of the reflected positioning signals are often rather limited in Ricean channel. Therefore, the interferences of the reflected positioning signals could be ignored. In Rayleigh channel, the powers of some multi-path components may be similar to the one of the strongest signal. So, the interferences of the positioning signals could not be ignored and the powers of the reflected positioning signals should be taken account into  $I(n)$ . However, if the positioning signals are much weaker than the environment noise, their interferences to the communication signals will be also ignored as  $I(n)$  will be much smaller than  $2N_0$ .

#### B. Interference of the Communication Signal to Positioning One

We assume length  $L$  spreading codes are used. Then, the positioning signal will be stronger than the communication one thanks to the spreading gain as long as the code length  $L$  is not too short. However, the communication signal compromises the performance of the range measuring. Because the positioning signal is continuous in the proposed MS-NOMA signal, the receiver can track the signal by a code-tracking loop. We assume BPSK modulation is used for the positioning signal, then the lower bound of the code phase estimation error in AWGN (Additive White Gaussian Noise) channel is [8]:

$$\sigma_{LB,m}^2 = \frac{a}{(2\pi)^2 \int_{B_0 - B_{fe}/2}^{B_0 + B_{fe}/2} f^2 \left[ \frac{P_{p,m} G_{p,m}(f)}{N_0 + NP_c G_c(f)} \right] df} \quad (3)$$

where  $a$  is determined by the loop parameters.  $B_0$  is the central frequency of MS-NOMA signal.  $B_{fe}$  is the double-sided front-end bandwidth.  $G_c(f)$  is the normalized PSD of the communication signal which satisfies  $G_c(f) = \frac{1}{N} \sum_{n=1}^N G_{c,n}(f)$ . Where  $G_{c,n}(f) = T_c \operatorname{sinc}^2[(f - n\Delta f_c)T_c]$  is the normalized PSD of the  $n^{\text{th}}$  C-User. Because the PSD of OFDM signal is approximately flat over the whole bandwidth [9]. We have  $G_c(f) \approx u_B(f - B_0)/B$ , where:

$$u_B(f) = \begin{cases} 1 & -\frac{B}{2} < f < \frac{B}{2} \\ 0 & \text{elsewhere} \end{cases} \quad (4)$$

Then (3) becomes:

$$\sigma_{LB,m}^2 = \frac{a}{(2\pi)^2} \left[ 2 \int_{B_{fe}/2}^{B/2} f^2 \frac{P_{p,m} G_{p,m}(f + m\Delta f_p)}{N_0} df + \int_{-B/2}^{B/2} f^2 \frac{P_{p,m} G_{p,m}(f + m\Delta f_p)}{N_0 + NP_c/B} df \right]^{-1} \quad (5)$$

By taking  $G_{p,m}(f)$  into (5), and using the approximation  $\operatorname{sinc}(BT_p) \approx \operatorname{sinc}(B_{fe}T_p) \approx 0$  (because of  $BT_p = M + 1 \gg 1$  and  $B_{fe} > B$ ), we obtain the simple

expression of  $\sigma_{LB,m}^2$ :

$$\sigma_{LB,m}^2 \approx 0.25aT_p^2 \frac{CPR_m}{E_b/N_0} \left( B_{fe} - \frac{E_b/N_0}{E_b/N_0 + 1} B \right)^{-1} \quad (6)$$

where  $E_b = P_c T_c$  is the energy of the communication symbol.  $CPR_m = \frac{\kappa P_c}{P_{p,m}}$  is defined as the communication-to-positioning ratio, where  $\kappa = 2G - 1 \approx 2G$  represents the amount of C-Users over one P-User's bandwidth ( $\approx$  is reasonable as  $\Delta f_p \gg \Delta f_c$ , i.e.,  $G \gg 1$ ). Notice that  $\frac{CPR_m}{E_b/N_0} = \frac{\kappa N_0}{T_c P_{p,m}}$  as well. So the first item in the brackets of (6) is the error caused by the environment noise and the second one is caused by the communication signal.

In the fading channel, the reflected communication signal will interfere the code phase estimation error as well. On the other hand, the reflected positioning signal will distort the auto-correlation function which may lead to estimation errors. In this letter, we do not consider the estimating biases caused by Non-Line of Sight (NLOS) as this is the common problem in all time based positioning system which has been discussed in plenty literatures. What we concern is the effect of the reflected communication signals rather than the positioning ones. Then, the tracking error of the Delay Locked Loop (DLL) is used to evaluate the tracking performance in the multi-path scenario.

Notice that there are multiple P-Users, i.e., the bandwidth of the positioning signal for one P-User (note as  $B_p$  for any P-Users) is much smaller than the total bandwidth  $B$ . Moreover, the front-end bandwidth is larger than  $B$  as well. So we have  $B_{fe} \gg B_p$ . Consequently, a DLL's narrow early-late spacing  $D$  can be applied.<sup>1</sup> Then, the  $S$  curve of DLL should be approximated to linear and the first-path of the positioning signal could be distinguished when  $D \rightarrow 0$ . So, the tracking error of DLL can be written as (7)<sup>2</sup> shown at the bottom of this page [8]. Where  $G_s(f)$  is the PSD of the received communication signal which may consist multi-path components.

In the practical use, (7) can be calculated by numerical integration as  $G_s(f)$  is usually complicated. (7) can be also analyzed by approximating a frequency non-selective slow fading channel to find the relationship between the range measurement accuracy and the signal's power. Then, we have  $G_s(f) \approx NP_c G_c(f) E(\alpha^2)$ , where  $\alpha$  is the normalized propagation amplitude which satisfies Ricean or Rayleigh distribution and  $E(\cdot)$  represents the mean value which satisfies  $E(\alpha^2) = \beta + \bar{P}_{c,\text{multi-path}}$ . Where  $\bar{P}_{c,\text{multi-path}}$  represents the normalized reflected communication signal's power. And  $\beta = 1$  or  $0$  in Ricean or Rayleigh channel, respectively. Notice that when  $D \rightarrow 0$ ,  $\sin(\pi f D T_p)$  in (7) can be replaced by Taylor expansion around 0. Then, by taking  $G_{p,m}(f)$  and  $G_c(f)$  into (7) and using the approximation  $\text{sinc}(BT_p) \approx$

<sup>1</sup>If  $B_{fe}$  is not large enough, the DLL correlation peak will be flattened which will deteriorate the performance of the phase discriminator.

<sup>2</sup>Taking the coherent early-late discriminator for example.

$\text{sinc}(B_{fe} T_p) \approx 0$ , after rearranging items, we have the simple expression of  $\sigma_{t,m}^2$  as:

$$\sigma_{t,m}^2 \approx 0.25aT_p^2 \left[ \frac{2}{B_{fe} T_p (P_{p,m}/N_0)} + \frac{B}{B_{fe}^2} CPR_m (\beta + \bar{P}_{c,\text{multi-path}}) \right] \quad (8)$$

where  $(P_{p,m}/N_0)$  is the carrier-to-noise ratio of the positioning signal over the  $m^{\text{th}}$  sub-carrier. The first item in (8) is caused by the noise, and the second one is caused by the communication signal. Particularly, if there are no multi-path signals, i.e.,  $\beta = 1$  and  $\bar{P}_{c,\text{multi-path}} = 0$ , (8) represents the DLL tracking error in AWGN channel which will converge to the lower bound  $\sigma_{LB,m}^2$ .

#### IV. PERFORMANCE EVALUATION

In this section, we evaluate the performances of the proposed MS-NOMA signal from two aspects - the BER and range measurement accuracy, respectively. The communication and positioning signals use QPSK and BPSK constellation, respectively. The positioning signal is 50 times faster than the communication one, i.e.,  $G = 50$ . The amount of P-User is  $M = 20$ , so that there are  $N = 1049$  C-Users. The powers of all C-Users are assumed as identical. The performances in both flat (AWGN) and fading channel are illustrated. Where the fading channel employs the Extended Typical Urban (ETU) model in 3GPP standard.

##### A. Communication Performance

We firstly examine the interference of the positioning signal to the C-Users. Figure 2(a) shows the average BERs over the whole bandwidth in both flat and fading channel when  $P_{p,m} = P_p, \forall m$ . It is clear that the average BERs decrease with the increasing of  $E_b/N_0$  ( $P_p/N_0$  as well). Notice that the BER curves with small CPRs will tend to be flat when  $E_b/N_0$  becomes larger (Region 2 in Figure 2(a)). This is because the interference caused by the positioning signal dominates the BER performance rather than the environment noise (i.e.,  $I(n)$  is much larger than  $2N_0$ ). When the positioning signal becomes weaker (CPR becomes larger), the BER curves will become flat with larger  $E_b/N_0$  and they will become closer to the one that only exists noise (CPR =  $\infty$ ). Moreover, the deterioration of the average BER in fading channel is much smaller than the one in the flat channel which means the interference of the superposed positioning signal could be ignored in this kind of scenario, especially with small  $E_b/N_0$ .

Figure 2(b) detailed shows the BERs for each C-User in flat channel. If the powers of the P-Users are identical (IPp), the BERs are approximately identical as well. While the BERs are different when the P-Users' powers are different (DPp). Then,

$$\sigma_{t,m}^2 = \frac{a \int_{-B_{fe}/2}^{B_{fe}/2} [N_0 + G_s(f)] G_{p,m}(f + m\Delta f_p) \sin^2(\pi f D T_p) df}{(2\pi)^2 P_{p,m} \left[ \int_{-B_{fe}/2}^{B_{fe}/2} f G_{p,m}(f + m\Delta f_p) \sin(\pi f D T_p) df \right]^2} \quad (7)$$

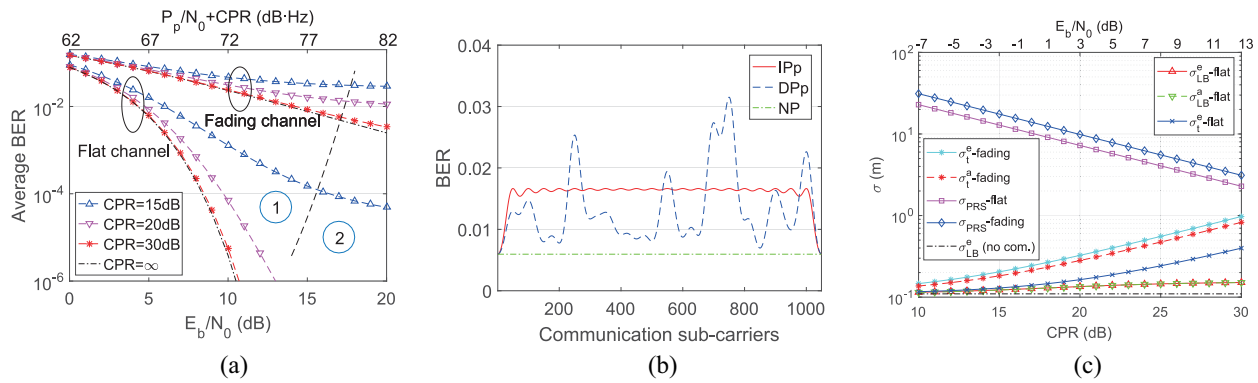


Fig. 2. Performance evaluation. (a) Average BER in different scenarios. (b) BER of the communication signal.  $E_b/N_0 = 5\text{dB}$ ,  $CPR = 15\text{dB}$ . (c) Range measurement accuracy at  $P_p/N_0 = 45\text{dB} \cdot \text{Hz}$ .

the maximum BER is related to all P-User's powers (see (1)) in this case. Of course, both of the Ipp and DPp are higher than the scenario that do not exist positioning signals (NP).

### B. Positioning Performance

We then examine the range measurement accuracy of the MS-NOMA signal. The front-end bandwidth is set to twice of the total bandwidth, i.e.,  $B_{fe} = 2B$ . The loop parameters are set as:  $B_L = 0.2\text{Hz}$ ,  $T_{coh} = 0.02\text{s}$  and  $D = 0.02\text{chips}$ , where  $B_L$  is the code loop noise bandwidth and  $T_{coh}$  is the predetection integration time. The range measurement accuracy of the MS-NOMA and PRS signal are compared. Where the lower bound of PRS is used as introduced in [10].

Figure 2(c) shows the range measurement accuracy when  $P_p/N_0 = 45\text{dB} \cdot \text{Hz}$ . Where superscript  $e$  and  $a$  represent the exact and approximate results, respectively. It is clear that the measurement errors of the MS-NOMA signal are always smaller than the ones of the PRS signal when  $CPR < 30\text{dB}$ . The accuracy gap between the two signals become larger when CPR decreases. It is because when the power of the communication signal decreases, its interference to the positioning one become weaker. While the measurement accuracy of PRS become worse due to the lower signal-to-noise ratio of the communication signal.

Please notice that the curves of the MS-NOMA signal will not change if the communication power is fixed and the positioning one is variable. For example, if  $E_b/N_0 = 0\text{dB}$  and  $P_p/N_0$  varies from  $32$  to  $52\text{dB} \cdot \text{Hz}$  (i.e.,  $10\text{dB} < CPR < 30\text{dB}$ ), the measurement accuracy of PRS is fixed at  $10.21\text{m}$  in AWGN channel and the accuracy of MS-NOMA is the same as Figure 2(c) shows. Then the measurement error will decrease when the power of the positioning signal increases.

On the other hand, the accuracy deterioration of MS-NOMA signal in fading channel become larger when the CPR increases. It is because the multi-path components multiply the affects of the CPR as (8) shown which means the stronger power of the positioning signal, the weaker effect of the channel fading. Although the relative accuracy deterioration of MS-NOMA signal in fading channel is a little larger than that of PRS, the absolute accuracy deterioration of MS-NOMA signal is much smaller than that of PRS.

Although stronger positioning power will have higher measurement accuracy and less channel fading effects (from the

angle of positioning), the maximum power of the positioning signals will be limited by the Quality of Service (QoS) of communication as Figure 2(a) and 2(b) show. In the real application,  $P_{p,m}$ s must be allocated carefully to acquire the best ranging performance under the QoS constraint which will be discussed in our future work.

Figure 2(c) also confirms that the approximations of both  $\sigma_{LB}$  and  $\sigma_t$  ((6) and (8)) correspond to the exact ones ((5) and (7)) very well. And all of them are below  $1\text{m}$  which ensures the meter level positioning accuracy compare to the  $10\text{m}$  level positioning accuracy of PRS. Meanwhile, the measurement error is only a little larger than the one that without communication signal, which means the effect of the communication signal is limit to the range measuring.

### REFERENCES

- [1] L. Yin, Q. Ni, and Z. Deng, "A GNSS/5G integrated positioning methodology in D2D communication networks," *IEEE J. Sel. Areas Commun.*, vol. 36, no. 2, pp. 351–362, Feb. 2018.
- [2] A. E. Assaf, S. Zaidi, S. Affes, and N. Kandil, "Robust ANNs-based WSN localization in the presence of anisotropic signal attenuation," *IEEE Wireless Commun. Lett.*, vol. 5, no. 5, pp. 504–507, Oct. 2016.
- [3] K. Medermott, R. M. Vaghefi, and R. M. Buehrer, "Cooperative UTDOA positioning in LTE cellular systems," in *Proc. GLOBECOM Workshops*, San Diego, CA, USA, 2016, pp. 1–6.
- [4] B. Sackenreuter, N. Hadaschik, M. Faßbinder, and C. Mutschler, "Low-complexity PDoA-based localization," in *Proc. Int. Conf. Indoor Position Indoor Navig.*, 2016, pp. 1–6.
- [5] Y. Liu, Z. Qin, M. El-kashlan, Y. Gao, and L. Hanzo, "Enhancing the physical layer security of non-orthogonal multiple access in large-scale networks," *IEEE Trans. Wireless Commun.*, vol. 16, no. 3, pp. 1656–1672, Mar. 2017.
- [6] B. Makki, T. Svensson, M. Coldrey, and M.-S. Alouini, "Finite block-length analysis of large-but-finite MIMO systems," *IEEE Wireless Commun. Lett.*, vol. 8, no. 1, pp. 113–116, Feb. 2019.
- [7] H. Hacı, H. Zhu, and J. Wang, "Performance of non-orthogonal multiple access with a novel asynchronous interference cancellation technique," *IEEE Trans. Commun.*, vol. 65, no. 3, pp. 1319–1335, Mar. 2017.
- [8] J. W. Betz and K. R. Kolodziejcki, "Generalized theory of code tracking with an early-late discriminator part I: Lower bound and coherent processing," *IEEE Trans. Aerosp. Electron. Syst.*, vol. 45, no. 4, pp. 1538–1556, Oct. 2009.
- [9] X. Tian, T. Zhang, Q. Zhang, and Z. Song, "High accuracy doppler processing with low complexity in OFDM-based RadCom systems," *IEEE Commun. Lett.*, vol. 21, no. 12, pp. 2618–2621, Dec. 2017.
- [10] J. A. Peral-Rosado, J. A. López-Salcedo, G. Seco-Granados, F. Zanier, and M. Crisci, "Joint channel and time delay estimation for LTE positioning reference signals," in *Proc. Satellite Navig. Technol. Eur. Workshop GNSS Signals Process.*, 2012, pp. 1–8.